Quest for dynamic topography: Observations from Southeast Asia

Paul Wheeler
Nicky White
Bullard Laboratories, Madingley Rise, Madingley Road, Cambridge CB3 0EZ, UK

ABSTRACT

Transient dynamic topography is maintained by time-varying density anomalies deep within Earth's mantle. There is considerable interest in predicting and measuring dynamic topography because its spatial and temporal variation will help to track changes in the pattern of mantle convection. Despite the availability of increasingly elaborate predictive models, there is little agreement about the amplitude, wavelength, and rate of change of dynamic topography. Here we analyze a hybrid data set of subsidence observations from continental and oceanic basins in Southeast Asia, where published dynamic models predict 1–2 km of regional subsidence. Residual subsidence was isolated by removing the well-defined effects of lithospheric extension and/or cooling. At long wavelengths (~10^3 km), the amplitude of residual subsidence (i.e., maximum permissible dynamic subsidence) has an upper bound of only ~300 m. The spatial distribution of permissible dynamic topography has no simple spatial or temporal relationship to the pattern of subduction over the past 65 m.y.; anomalous subsidence commenced 5–10 m.y. ago, accelerating to a present-day rate of ~100 m/m.y. Our results show that density anomalies within the lower mantle have little apparent influence at Earth's surface. Instead, the distribution of residual subsidence reported here can be accounted for by minor variations in lithospheric thickness or by transient density variations beneath the lithospheric plate. The absence of measurable dynamic topography is surprising and indicates that mantle mass anomalies are supported elsewhere, presumably at internal boundaries within Earth. Our hybrid data set can thus be used as an independent constraint on the viscosity structure of the mantle.

Keywords: dynamic topography, basin, Southeast Asia.

PREDICTION AND MEASUREMENT OF DYNAMIC TOPOGRAPHY

Spatial and temporal variations of topography on Earth are balanced by isostatic compensation at the base of the lithosphere. In the oceans, the slow subsidence of seafloor away from mid-oceanic ridges is almost exclusively governed by cooling and thickening of the lithospheric plate (Parsons and Sclater, 1977). Prominent short-wavelength (~10^2 km) features, such as plateaus and seamounts, are regionally compensated by plate flexure and by magmatic underplating. In contrast, continental topography is predominantly supported by variations in crustal thickness and density. A globally important exception is lithospheric stretching when regional subsidence caused by crustal thinning is modulated by the growth and decay of a thermal anomaly (Jarvis and McKenzie, 1980). Thus, despite the obvious importance of transient dynamic topography controlled by deep mantle processes, isolating an unambiguous signal, particularly on the continents, has proven to be a difficult challenge.

However, rapid progress has been made in developing global models that predict dynamic topography (Hager and Clayton, 1989; Lithgow-Bertelloni and Gurnis, 1997; Ricard et al., 1993; Mitrovica et al., 1989). The starting point is the density distribution within the mantle, usually estimated from seismic tomographic results or from the history of subduction. Assuming knowledge of the viscosity structure of the mantle, this density distribution is used to calculate the shape of deformable interfaces, notably the core-mantle boundary and Earth's surface (Parsons and Daly, 1983; Hager, 1984). The largest amplitudes are expected to occur close to active subduction zones, and so the best-constrained models are for Southeast Asia (Lithgow-Bertelloni and Gurnis, 1997; Ricard et al., 1993; Fig. 1). The

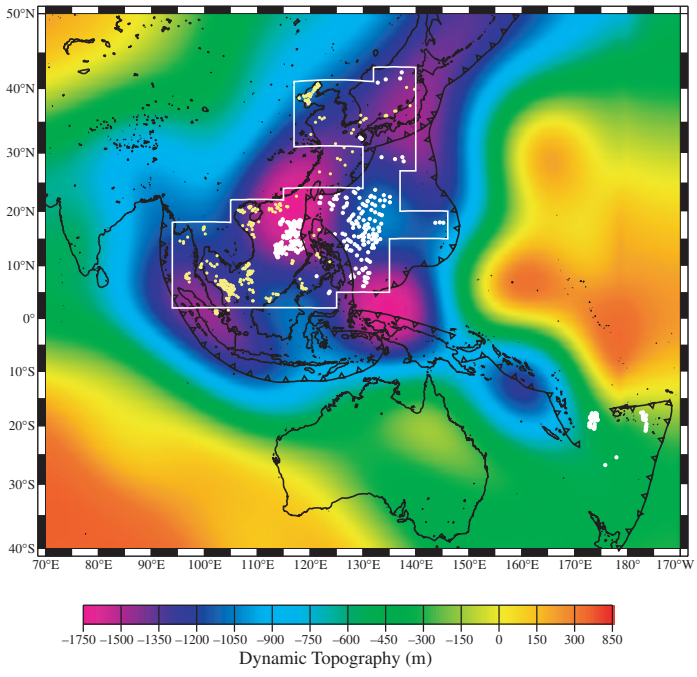

Figure 1. Map of predicted dynamic topography for Southeast Asia calculated by Lithgow-Bertelloni and Gurnis (1997), using history of subduction over past 180 m.y. (see also Ricard et al., 1993). Cold colors indicate dynamic subsidence, and warm colors indicate dynamic uplift. In Lithgow-Bertelloni and Gurnis model, subducted slabs sink vertically and form main source of density variation within mantle. Slab density as function of age was estimated using Parsons and Sclater's (1977) results. Given this density field, they solve equations of motion for incompressible Newtonian fluid together with Poisson's equations for gravitational potential. Amplitude and wavelength of predicted geoid and dynamic topography are both sensitive to mantle's viscosity structure. Other researchers have obtained similar results for Southeast Asia using density distributions based upon results of seismic tomography. Region outlined in white is focus of our study: solid white circles—417 age-depth measurements from marginal oceanic basins; solid yellow circles—353 boreholes from continental sedimentary basins.

global variation of predicted dynamic topography remains poorly defined as a result of large uncertainties in mantle density distribution.

For a given density distribution, the amplitude and sign of predicted dynamic topography are strongly dependent upon the viscosity structure of the mantle (Hager, 1984). Thus, it is essential to use independent observations to test any dynamical prediction. The most reliable methods isolate subsidence anomalies that cannot be accounted for by generally accepted plate cooling and stretching models. These anomalies could have various causes and at this stage should only be used to bound the maximum possible dynamic signal. The most thorough work has been carried out in the oceans, where residual bathymetry can be measured with ease. On older oceanic lithosphere, long-wavelength swells with amplitudes of ~200 m are clearly identifiable, although there is some debate about their significance (Colin and Fleitout, 1990; Cazenave and Lago, 1991). A correlation at degree two between residual bathymetry and the geoid favors a relationship to mantle convection. This interpretation is complicated by evidence for a very low viscosity layer ($\eta \sim 10^{19}$ Pa·s) at the base of the oceanic lithosphere (Craig and McKenzie, 1986; Robinson et al., 1987). Furthermore, data from the oceans will always be of limited use, because we can only measure the present-day response.

On the continents, dynamic topography has proved to be elusive, although the detailed stratigraphic record is potentially valuable because it contains both spatial and temporal information. The simplest approach exploits the degree to which continents are flooded over geologic time (Gurnis, 1990, 1993). Although flooding rates have yielded some general insights, a detailed analysis is fraught with difficulties unless the continent-wide effects of thermally driven subsidence are first removed. Phanerozoic subsidence data from continental interiors (Bond and Kominz, 1991; Burgess and Gurnis, 1995) are more useful, but the predictive power of dynamic models is considerably degraded by a lack of information about ancient mantle density variations. Continental data can only be exploited by first removing the almost ubiquitous effects of rifting.

ANALYSIS OF A HYBRID DATA SET

Most of these difficulties can be circumvented by exploiting a combination of observations from young oceanic and continental basins in Southeast Asia, where the greatest amount of present-day dynamic subsidence has been consistently predicted. The excess mantle density that drives dynamic subsidence has been generated by subduction over the past 65 m.y. Thus, the spatial and temporal evolution of predicted dynamic topography is well founded, at least in broad terms. The tectonic framework of Southeast Asia is dominated by the formation of extensional sedimentary basins and marginal oceanic basins, whose subsidence behavior can be accurately predicted using well-known models.

We first reanalyzed age-depth data from marginal oceanic basins (Fig. 2A). Original ship tracks were examined in conjunction with magnetic anomalies rather than using global bathymetric compilations, which are much less accurate (e.g., ETOPO5). We have corrected for sediment loading but not for crustal thickness variation, which is poorly known. In the areas examined, oceanic crust is generally thinner than 7 km, and so the subsidence anomalies in Figure 2A should be regarded as absolute maxima. Results demonstrate the anticipated increase of depth with age, although there is considerable scatter. Active marginal basins have age-depth anomalies that range from –1200 m to +700 m. In some cases, such as the Lau basin, it is clear that residuals reflect variations in crustal thickness (Turner et al., 1999). The older marginal basins have greater than expected depths. In the South China Sea, age-depth picks occur below the global relationship, although they are within two standard deviations of the North Pacific mean. Limited evidence suggests that oceanic crust is as thin as 5 km in places (Spangler-Nissan et al., 1995), yielding a maximum of ~200 m of residual

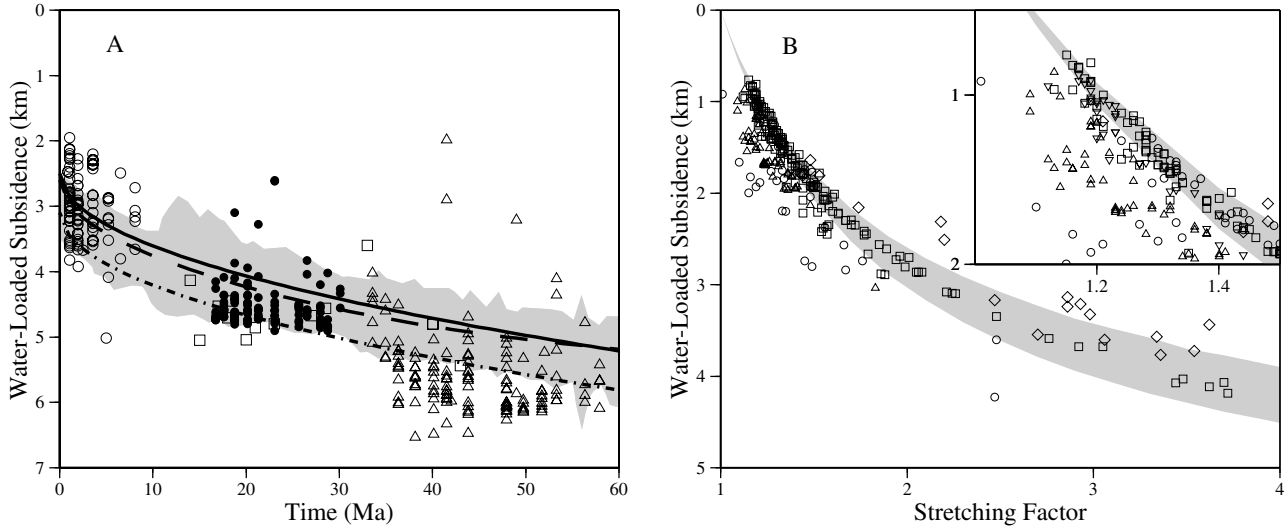

Figure 2. A: Water-loaded subsidence as function of age for marginal oceanic basins calculated using NGDC Geodas marine trackline geophysics database and Ocean Drilling Program wells (417 points). Ages of oceanic crust were determined using magnetic anomalies, and depths have been corrected for sediment thicknesses. Open circles—actively spreading basins (Lau, North Fiji, Marianas, and Scotia); solid circles—South China Sea; open triangles—Philippine Sea; squares—other areas (Japan, Celebes, Shikoku, South Fiji, and Sulu Seas). Shaded zone shows two standard deviations about North Pacific average. Solid and dashed lines are global relationships based upon plate cooling model with 7-km-thick crust (Parsons and Sclater, 1977, and Stein and Stein, 1992, respectively). Dot-dash line is Parsons and Sclater curve with 4-km-thick crust. B: Water-loaded subsidence as function of lithospheric stretching factor, β, for continental sedimentary basins fringing marginal oceanic basins (279 boreholes). Squares—Oligocene rift basins on Sundaland shelf (Malay, Gulf of Thailand, Natuna, and Sarawak); circles—late Eocene–Oligocene rift basins offshore Vietnam (Mekong, Nam Con Son, Yinggehai, Qiong Dong Nan, and Tonking); triangles—Paleocene rift basins offshore North China (Bohai and Yellow Sea); inverted triangles—Paleocene rift basins offshore South China (Pearl River Mouth and Beibu); diamonds—Oligocene rift basins that were recently uplifted and denuded (Japan Sea and Mergui). Shaded zone delimits behavior consistent with lithospheric rifting and consequent thermal subsidence; upper boundary represents Oligocene rifting (33–20 Ma); lower boundary represents Paleocene rifting (60–30 Ma). Inset is enlargement of top left corner. Anomalously low subsidence falls above shaded zone and occurs in basins with recent uplift and denudation. Anomalously high subsidence falls below shaded zone and could represent dynamic subsidence.

subsidence. The largest residual subsidence occurs in the Philippine Sea, although estimates must be corrected for crustal thicknesses that could be as low as 4 km in the Parece Vela basin (Sclater et al., 1976). A reasonable upper bound for residual subsidence is 300 m.

Fortunately, these marginal oceanic basins are all younger than 60 Ma, and so subsidence anomalies are not affected by conflicting dynamic interpretations of age-depth flattening (Colin and Fleitout, 1990; Cazenave and Lago, 1991). Nevertheless, these static observations are of limited value on their own. Stratigraphic information from deep boreholes probably provide the best means for determining the spatial and, more important, the temporal variation of residual subsidence. We have collated and digitized 353 stratigraphic sections from boreholes throughout Southeast Asia (Figs. 1 and 2B). These data span the past 60 m.y. and are from extensional basins where the stratigraphic sequence is as complete as possible. We have not included foreland basins in our analysis, because isolating anomalous subsidence in these cases is less easy. Tectonic subsidence for each well was calculated and modeled using an inverse algorithm to determine extensional strain rate variation (White, 1993). Data inversion yields excellent fits between theoretical and observed subsidence, and strain-rate profiles are consistent with independent geological information about the number and duration of rift episodes (Fig. 3A–3E). Our results are not significantly changed when a range of lithospheric and crustal thicknesses are used. Uncertainties in the thermal structure of the lithosphere can be explicitly included in the inversion algorithm (Newman and White, 1999). It is evident that modest amounts of rifting occurred in the early and/or middle Cenozoic ($\beta \sim 1.2$). Where possible, we have also carried out two-dimensional inverse modeling of interpreted and depth-converted seismic reflection profiles (Fig. 3F–3J). Our two-dimensional results demonstrate that the flexural rigidity of these extensional basins is very low, validating the more comprehensive one-dimensional analysis (see Bellingham and White, 2000).

In contrast to the oceanic data, the bulk of our subsidence data shows no evidence for anomalous subsidence (Fig. 2B). Where anomalies are evident, they are generally ~300 m, although outliers with residuals of ~1 km of water-loaded subsidence sometimes occur. Our results show that anomalous subsidence is confined to the past 10 m.y.; there is no evidence for any anomalous events earlier in the Cenozoic. Rates vary from 50 to 150 m/m.y. and generally increase toward the present day (e.g., Fig. 3C and 3D). These results are robust to changes in strain rate regularization and input parameterization.

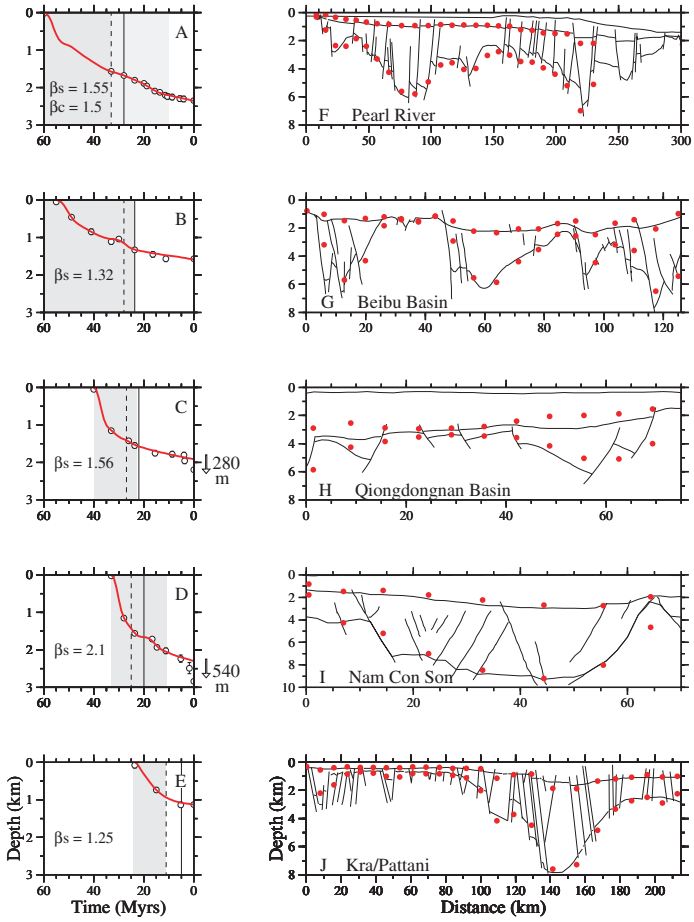

Figure 3. A–E: Results of modeling five stratigraphic sections derived from boreholes in sedimentary basins (named in right plots). Tectonic (i.e., water loaded) subsidence (circles) was produced by standard decompaction and backstripping. Errors in water depth through time are minimal because sediments are either lacustrine or shallow marine. Solid line—best-fitting theoretical subsidence curve obtained by one-dimensional inversion (algorithm inverts for lithospheric strain rate as function of time; see White [1993] for further details and values of constants). Periods of lithospheric rifting, indicated by shaded zones, were independently estimated using interpreted seismic reflection data (15 000 km). β_s—subsidence-derived stretching factor; β_c—crustal-derived stretching factor (Spangler-Nissan et al., 1995). Dashed vertical line—first marine incursion; solid vertical line—onset of fully marine conditions. Note how onset of marine conditions is related to rift timing and magnitude. Amplitude of anomalous water-loaded subsidence is given for C and D. F–J: Results of modeling two-dimensional profiles that cross each basin. Slanted lines—normal faulting demonstrating existence of crustal extension; three horizons—bottom of basin, end of main rifting, and sea bed. For G, I, and J, sea bed is indistinguishable from 0 km at this scale. Solid circles—best-fitting theoretical profiles obtained by two-dimensional inversion. Two-dimensional algorithm, written by Paul Bellingham, inverts for lithospheric strain rate as function of time and space and includes features such as lithospheric flexure and two-dimensional heat flow. Optimization indicates that effective elastic thickness cannot be greater than 2 km (see Bellingham and White [2000] for further details and values of constants).

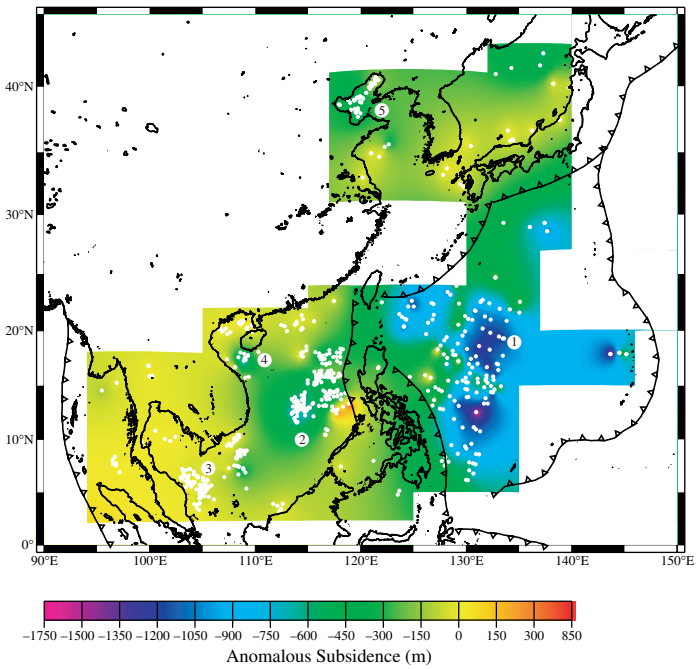

Figure 4. Spatial distribution of anomalous subsidence within highlighted region of Figure 1; 678 picks (solid white circles) from Figure 2 were used. Prominent seamounts are excluded. Gridding and interpolation was carried out using generic mapping tools; to aid comparison, color scale is same as in Figure 1. Amplitudes are generally ≤300 m; obvious exception is Philippine Sea, where spatial pattern mimics bathymetry. 1—Northwest Philippine basin; 2—South China Sea; 3—Sundaland Shelf; 4—Yinggehai basin; 5—Bohai basin.

The combined oceanic and continental results suggest that the maximum possible residual subsidence in southeast Asia is ~300 m. This amount is nearly one order of magnitude smaller than the predicted dynamic topography. A more obvious source of discrepancy is the spatial distribution of this residual subsidence (Fig. 4). Most of the significant anomalies are in oceanic basins where crustal thicknesses are relatively poorly known. The Philippine Sea residuals match basin physiography, which suggests that crustal thickness variations play an important role in generating age-depth anomalies. In the fringing extensional basins, the largest residuals are confined to specific areas such as the Yinggehai basin, close to Hainan Island, and the Bohai basin, offshore North China. We note that both of these basins have evolved close to substantial strike-slip faults; movement on them has affected basin development.

IMPLICATIONS OF NEGLIGIBLE DYNAMIC SIGNATURE

Despite our attempts to maximize possible estimates of dynamic subsidence, two independent data sets suggest that any dynamic signal has a considerably smaller amplitude than predicted. Much more important is that a detailed comparison of Figures 1 and 4 shows that there is no obvious relationship between predicted and observed wavelengths; in general, a negative correlation is evident. The development of residual subsidence shows that any dynamic subsidence cannot have developed in concert with Cenozoic subduction.

How can these important differences be explained? As Hager (1984) pointed out, it is unlikely that the mass excess within the mantle beneath Southeast Asia has been seriously overestimated; otherwise, it would be difficult to fit the geoid. The most poorly defined feature of dynamical calculations is the variation of mantle viscosity with depth. If the viscosity directly beneath the lithosphere is decreased by several orders of magnitude, the amplitude of dynamic topography at Earth's surface is reduced, but only by ~20% (Lithgow-Bertelloni and Gurnis, 1997). Negligible dynamic topography can be generated only if the buoyancy forces are supported exclusively at deeper levels within the mantle (Wen and Anderson, 1997). Our results thus place an important upper bound on mantle viscosity structure. A global analysis of residual subsidence and uplift that jointly exploits oceanic and continental data should yield fruitful insights.

ACKNOWLEDGMENTS

Wheeler was supported by an Arco-funded studentship. Well log and seismic data were generously provided by Arco, BP-Amoco, Lasmo, and Shell. We are very grateful to P. Bellingham for allowing us to show results from his unpublished two-dimensional basin inversion software. We thank S. Bergman, S. Booth, P. Faulkner, B. Lovell, D. Lyness, S. Jones, D. McKenzie, and J. Toth for their help. Cambridge Earth Sciences contribution 6015.

REFERENCES CITED

Bellingham, P., and White, N., 2000, Spatial and temporal variation in strain rate from 2D inversion of subsidence data: Basin Research (in press).

Bond, G., and Kominz, M., 1991, Disentangling Middle Paleozoic sea-level events in cratonic basins and cratonic margins of North America: Journal of Geophysical Research, v. 96, p. 6619–6639.

Burgess, P., and Gurnis, M., 1995, Mechanism for the formation of cratonic stratigraphic sequences: Earth and Planetary Science Letters, v. 136, p. 647–663.

Cazenave, A., and Lago, B., 1991, Long wavelength topography, sea-floor subsidence and flattening: Geophysical Research Letters, v. 18, p. 1257–1260.

Colin, P., and Fleitout, L., 1990, Topography of the ocean floor: Thermal evolution of the lithosphere and interaction of mantle heterogeneities with the lithosphere: Geophysical Research Letters, v. 11, p. 1961–1964.

Craig, C., and McKenzie, D., 1986, The existence of a thin low-viscosity layer beneath the lithosphere: Earth and Planetary Science Letters, v. 78, p. 420–426.

Gurnis, M., 1990, Bounds on global dynamic topography from Phanerozoic flooding of continental platforms: Nature, v. 344, p. 754–756.

Gurnis, M., 1993, Dynamic surface topography: A new interpretation based upon mantle flow models derived from seismic topography: Comment: Geophysical Research Letters, v. 20, p. 1663–1664.

Hager, B., 1984, Subducted slabs and the geoid: Constraints on mantle rheology and flow: Journal of Geophysical Research, v. 89, p. 6003–6015.

Hager, B., and Clayton, R., 1989, Constraints on the structure of mantle convection using seismic observations, flow models and the geoid, *in* Peltier, W.R., ed., Mantle convection: Plate tectonics and global dynamics: New York, Gordon and Breach, p. 657–763.

Jarvis, G., and McKenzie, D., 1980, Sedimentary basin formation with finite extension rates: Earth and Planetary Science Letters, v. 48, p. 42–52.

Lithgow-Bertelloni, C., and Gurnis, M., 1997, Cenozoic subsidence and uplift of continents from time-varying dynamic topography: Geology, v. 25, p. 735–738.

Mitrovica, J., Beaumont, C., and Jarvis, G., 1989, Tilting of continental interiors by the dynamical effects of subduction: Tectonics, v. 8, p. 1079–1094.

Newman, R., and White, N., 1999, The dynamics of extensional sedimentary basins: Constraints from subsidence inversion: Royal Society of London Philosophical Transactions: v. 357, p. 805–834.

Parsons, B., and Daly, S., 1983, The relationship between surface topography, gravity anomalies, and the temperature structure of convection: Journal of Geophysical Research, v. 88, p. 1129–1144.

Parsons, B., and Sclater, J., 1977, An analysis of the variation of ocean floor bathymetry and heat flow with age: Journal of Geophysical Research, v. 82, p. 803–827.

Ricard, Y., Richards, M., Lithgow-Bertelloni, C., and Le Stuenff, Y., 1993, A geodynamic model of mantle density heterogeneity: Journal of Geophysical Research, v. 98, p. 21,895–21,909.

Robinson, E.M., Parsons, B., and Daly, S., 1987, The effect of a shallow low viscosity zone on the apparent compensation of mid-plate swells: Earth and Planetary Science Letters, v. 82, p. 335–348.

Sclater, J., Karig, D., Lawver, L., and Louden, K., 1976, Heat flow, depth and crustal thickness of the marginal basins of the South Philippine Sea: Journal of Geophysical Research, v. 81, p. 309–318.

Spangler-Nissan, S., Hayes, D., Yao Bochu, Zeng Weijun, Chen Yongqin, and Nu Xiaupin, 1995, Gravity, heat flow, and seismic constraints on the processes of crustal extension: Northern margin of the South China Sea: Journal of Geophysical Research, v. 100, p. 22,447–22,483.

Stein, C., and Stein, S., 1992, A model for the global variation in oceanic depth and heat flow with lithospheric age: Nature, v. 359, p. 123–128.

Turner, I., Pierce, C., and Sinha, M., 1999, Seismic imaging of the axial region of the Valu Fa Ridge, Lau Basin—The accretionary processes of an intermediate back-arc spreading ridge: Geophysical Journal International, v. 138, p. 495–519.

Wen, L., and Anderson, D., 1997, Layered mantle convection: A model for geoid and topography: Earth and Planetary Science Letters, v. 146, p. 367–377.

White, N., 1993, Recovery of strain rate variation from inversion of subsidence data: Nature, v. 366, p. 449–452.

Manuscript received April 3, 2000
Revised manuscript received July 17, 2000
Manuscript accepted August 6, 2000